

Determination of the size, mass, and density of “exomoons” from photometric transit timing variations

A. Simon¹, K. Szatmáry¹ and Gy. M. Szabó^{1,2}

¹ Department of Experimental Physics & Astronomical Observatory, University of Szeged, 6720 Szeged, Hungary

² Magyary Zoltán Research Fellow

e-mail: asimon@titan.physx.u-szeged.hu

ABSTRACT

Aims. Precise photometric measurements of the upcoming space missions allow the size, mass, and density of satellites of exoplanets to be determined. Here we present such an analysis using the photometric transit timing variation (TTV_p).

Methods. We examined the light curve effects of both the transiting planet and its satellite. We define the photometric central time of the transit that is equivalent to the transit of a fixed photocenter. This point orbits the barycenter, and leads to the photometric transit timing variations.

Results. The exact value of TTV_p depends on the ratio of the density, the mass, and the size of the satellite and the planet. Since two of those parameters are independent, a reliable estimation of the density ratio leads to an estimation of the size and the mass of the exomoon. Upper estimations of the parameters are possible in the case when an upper limit of TTV_p is known. In case the density ratio cannot be estimated reliably, we propose an approximation with assuming equal densities. The presented photocenter TTV_p analysis predicts the size of the satellite better than the mass. We simulated transits of the Earth-Moon system in front of the Sun. The estimated size and mass of the Moon are 0.020 Earth-mass and 0.274 Earth-size if equal densities are assumed. This result is comparable to the real values within a factor of 2. If we include the real density ratio (about 0.6), the results are 0.010 Earth-Mass and 0.253 Earth-size, which agree with the real values within 20%.

Key words. Planets and satellites: general - Methods: data analysis - Techniques: photometric

1. Introduction

The discovery of planets in other solar systems (“exoplanets”) led to the question of whether these planets also have satellites (“exomoons”). The photometric detection of such a satellite was first suggested by Sartoretti & Schneider (1999, SS99 in the followings; also discussed by Deeg, 2002), who gave a method for estimating the mass of this exomoon. The idea is to calculate the barycentric transit timing variations (TTV_b). This quantity has been applied to the upper mass estimations of hypothetical satellites around transiting exoplanets (Charbonneau et al. 2005; Bakos et al. 2006; McCullough et al. 2006; Steffen et al. 2005; Gillon et al. 2006). In this theory, the barycenter orbits the star with a constant velocity, and it transits strictly periodically. As the planet (and the satellite, too) revolves around the planet-satellite barycenter, the transit of the planet wobbles in time. The TTV_b is based on finding the center between ingress/egress or from some other method known from eclipse minimum timing. The circular velocity around the star can be expressed via

the m_* mass of the star and the a_p semi-major axis of the planet as $v = \sqrt{\frac{\gamma m_*}{a_p}}$. The maximal normal amplitude (i.e. half of the peak-to-peak amplitude) is finally

$$\text{TTV}_b = \frac{1}{v} B_c, \quad (1)$$

where $B_c = \frac{a_s m_s}{m_p + m_s}$ is the distance from the centerpoint of the planet to the barycenter. Here a_s is the semi-major axis of the satellite, and $m_s < m_p$ are the mass of the satellite and the planet, respectively. If TTV_b is observed or if there is an upper limit, the mass is estimated by setting a_s to the borders of Hill-stable regions, $a_s = a_H \equiv a_p \left(\frac{m_p}{3m_*}\right)^{1/3}$ the Hill-radius. With this selection, m_s remains the single parameter and it can be determined as

$$m_{s,SS99} = \frac{v \text{TTV}_b}{a_s} m_p = \frac{v \text{TTV}_b}{a_p} (3m_p^2 m_*)^{1/3} \quad (2)$$

(Eq. (24) in SS99). This model can be refined by including the results of Barnes and O’Brien (2002), who suggests more stringent constraints on the survivability of

exomoons: the maximal distance from the planet is about $a_H/3$, depending slightly on the mass ratio. More recently, Domingos et al. (2006) have suggested that the maximum semimajor axis is $0.4895a_H$ for a prograde satellite and is $0.9309a_H$ for a retrograde satellite, both in circular orbit and with a mass ratio $m_s/m_p = 0.001$. With the realistic choice of $a_s = a_H/3$, the satellite masses would lead to better estimates that are about three times larger than given by Eq. 2. However, this modification has been rarely adopted in the literature.

In Szabó et al (2006) we designed numerical simulations to predict how probable the discovery of an exomoon is with a photometric technique. For this detection we suggested using the (photometric) central time of the transit, τ as

$$\tau = \frac{\sum t_i \Delta m_i}{\sum \Delta m_i}, \quad (3)$$

where m_i is the i -th magnitude measurement at t_i time. We show later the *photometric transit timing variation*, TTV_p calculated from this τ requires its own physical interpretation, which differs from the conventional TTV_b . The difference is to account for the photometric effects of *both* the planet and the satellite: even when the satellite cannot be detected directly in the light curve, its presence can actually dominate TTV_p . We have shown that τ is robust, therefore it is applicable even in the case of as “noisy” data series as the COROT and Kepler missions provide. These missions are able to detect a Moon-like satellite around an Earth-like planet with 20% probability (Szabó et al., 2006).

In this paper we give the complete analytical description of this theory of photometric timings, directly leading to estimation of various parameters such as the mass and the radius of the satellite. We test the formulae by modeling the Earth-Moon system.

2. Light curve morphology

Let us assume a planet and its satellite transiting the star. The position of the planet and the satellite is such that their images do not overlap as seen by the observer. We then assume that the relative position of the planet and the satellite does not change during the transit; the transit is central and the orbital inclination of the satellite is 0. Let the sampling of the light curve be uniform. Under these assumptions, τ is exactly the barycenter of the light curve (i.e. considered as a polygon). Furthermore, let

$$\mu = m_s/m_p, \quad \chi = \rho_s/\rho_p, \quad \vartheta = r_s/r_p \quad (4)$$

be the ratio of the masses, densities and sizes (radii), respectively. Any of the three can be expressed from the two other ones. In the case of the direct detection of the satellite in the shape of the light curve, one can directly calculate $\vartheta^2 = \Delta m_s/\Delta m_p$, where Δm_s and Δm_p are the brightness decreases due to the satellite and the planet, respectively. But even if the noise level is too high for a direct detection, the presence of a moon can be reasoned

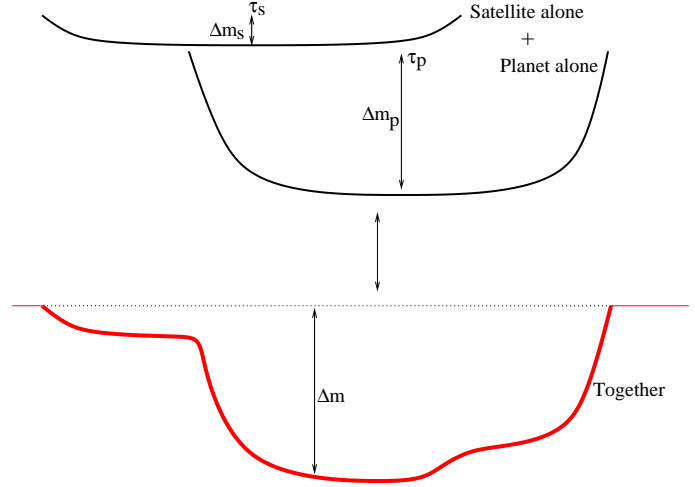


Fig. 1. Composition of the transit light curve from Δm_p and Δm_s .

indirectly (Szabó et al. 2006), as formulated in the following.

The shape of the light curve is the sum of two components: a single planet and a single moon in transit (Fig. 1). The shape of those components is

$$\Delta m_{s,ti} = \frac{r_s^2}{r_*^2} f(t_i - \tau_s), \quad (5)$$

$$\Delta m_{p,ti} = \frac{r_p^2}{r_*^2} f(t_i - \tau_p), \quad (6)$$

where $\Delta m_{s,ti}$ and $\Delta m_{p,ti}$ are the magnitude decreases at time t_i , and τ_p and τ_s are the times when the planet and the satellite each passes alone before the central meridian of the star. Here $f(x)$ is the normalized shape function of the transit. We can assume that $f(x)$ is an axially symmetric light curve to $x = 0$, and its off-transit value is 0.

If we consider the transit of the planet and the moon together,

$$\Delta m_i = \Delta m_{s,ti} + \Delta m_{p,ti}. \quad (7)$$

In this case we know from Eqs. 3 and 7 that

$$\tau = \frac{\sum t_i \Delta m_{p,ti} + \sum t_i \Delta m_{s,ti}}{\sum \Delta m_i}. \quad (8)$$

Let $N = \sum f(t_i)$ be the “area” under the function f . With this, we can easily rewrite the nominator as

$$\sum \Delta m_i = \frac{r_s^2 + r_p^2}{r_*^2} N. \quad (9)$$

Taking the axial symmetry of f into account, the numerator of Eq. 8 can be similarly rewritten as

$$\sum t_i \Delta m_{s,ti} + \sum t_i \Delta m_{p,ti} = \frac{r_s^2}{r_*^2} N \cdot \tau_s + \frac{r_p^2}{r_*^2} N \cdot \tau_p, \quad (10)$$

and finally

$$\tau = \frac{\frac{r_s^2}{r_*^2} N \cdot \tau_s + \frac{r_p^2}{r_*^2} N \cdot \tau_p}{\frac{r_s^2 + r_p^2}{r_*^2} N} = \frac{r_s^2 \tau_s + r_p^2 \tau_p}{r_s^2 + r_p^2}. \quad (11)$$

Now let us consider an extreme configuration with a leading moon. We consider the first contact time, when the ingress of the satellite begins, and relate it to the time when the satellite is exactly in the center of the stellar disc. Between these events, $\tau_s = \frac{1}{v}(r_s + r_*)$ time has to elapse. The time between the first contact of the satellite and the time when the planet is in front of the center of the stellar disc is $\tau_p = \frac{1}{v}(r_s + r_* + a_s)$. Substituting these and the analogous formulae into Eq. 11,

$$\tau = \frac{1}{v} \left(r_s + \frac{a_s r_p^2}{r_s^2 + r_p^2} + r_* \right) \quad (12)$$

with a leading satellite and

$$\tau = \frac{1}{v} \left(r_p + \frac{a_s r_s^2}{r_s^2 + r_p^2} + r_* \right) \quad (13)$$

with a trailing satellite.

The basic conclusion is that the planet-satellite system can be substituted by a single celestial body, which can cause the same TTV_p and which is located on the planet-moon line at $P_c = a_s \frac{r_s^2}{r_s^2 + r_p^2}$ distance from the planet. We call this particular point as “*photocenter*” in the following.

The barycenter lies at $B_c = \frac{a_s m_s}{m_s + m_p}$ distance from the planet and it revolves strictly periodically. The photocenter lies somewhere else between the planet and the satellite, therefore the τ time of the transit will wobble in time (See Fig. 2). The time between the transit of the barycenter and the photocenter is TTV_p , which can be expressed as

$$\text{TTV}_p = \frac{1}{v} |P_c - B_c| = \frac{1}{v} \left| \frac{a_s r_s^2}{r_p^2 + r_s^2} - \frac{a_s m_s}{m_p + m_s} \right| = \frac{a_s}{v} \left| \frac{\vartheta^2}{1 + \vartheta^2} - \frac{\mu}{1 + \mu} \right|. \quad (14)$$

With neglecting ϑ^2 and μ to 1 ($\vartheta^2 \ll 1$, $\mu \ll 1$, their values $\lesssim 0.01$) in the nominators, TTV_p simplifies to our basic equation

$$\text{TTV}_p = \frac{a_s}{v} |\vartheta^2 - \mu|, \quad (15)$$

where $\mu = m_p/m_s$ is the mass ratio and $\vartheta = r_s/r_p$ the ratio of radii. The comparison of Eqs. 1 and 14 shows the difference between the SS99-theory and the present approach: the introduction of the P_c term. This reflects the different basic concepts. In the SS99-theory, TTV_b is a dynamical timing effect caused by the revolution of the planet around the barycenter. In our present approach, TTV_p is due to the revolution of the photocenter, which both combines the dynamical and the photometrical properties of the moon and offers a potential to estimate the mass and the size of the satellite.

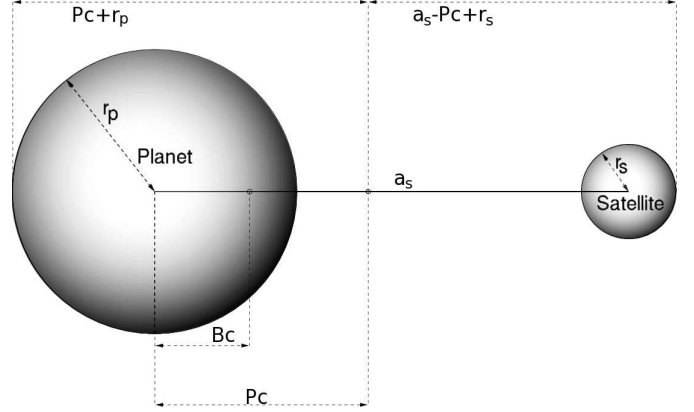


Fig. 2. Position of the barycenter and the photocenter in a transiting system (not to scale).

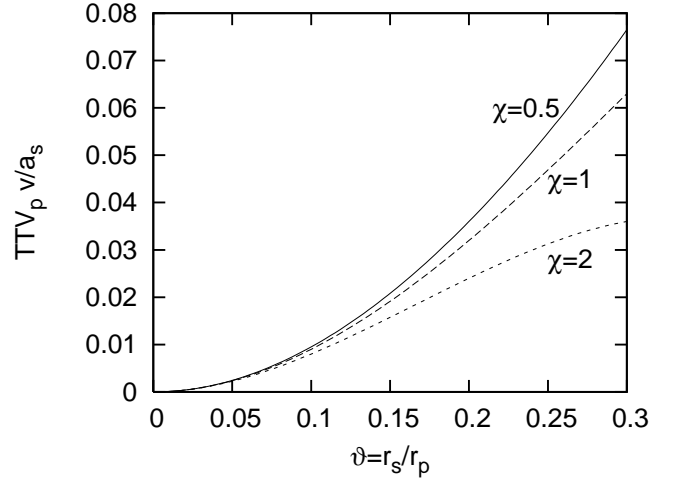


Fig. 3. The dependence of TTV_p (multiplied by the term v/a_s) on the size ratio. The three different curves show three satellites with different density ratios.

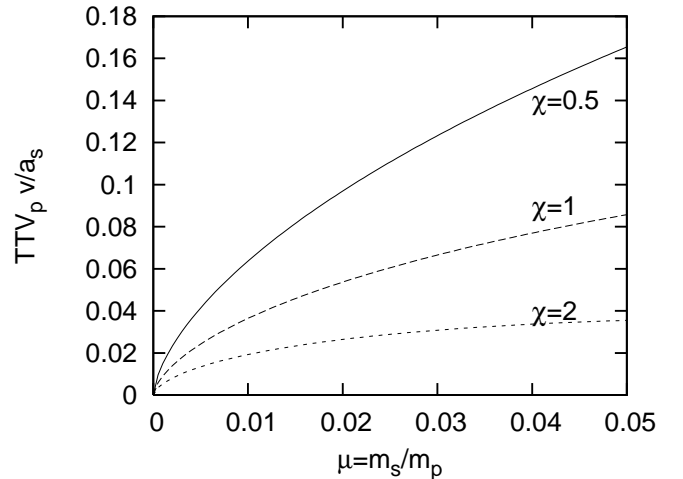


Fig. 4. The same as Fig. 3 but for the mass dependence. Note that TTV_p depends noticeably on the density in this model, which makes the mass determination more ambiguous.

2.1. Expressions for the radius and mass of the moon

By expressing the mass ratio μ through the radii r_p , r_s and the densities ρ_p , ρ_s in Eq. 15, we get the formula for the size ratio ϑ :

$$\text{TTV}_p = \frac{a_s}{v} \frac{r_s^3}{r_p^3} \left| \frac{r_p}{r_s} - \frac{\rho_s}{\rho_p} \right| = \frac{a_s}{v} \left| \frac{1}{\vartheta} - \chi \right| \vartheta^3, \quad (16)$$

$$\Delta \text{TTV}_p = \frac{a_s}{v} \{ [2\vartheta - 3\vartheta^2\chi] \Delta\vartheta - \vartheta^3 \Delta\chi \}. \quad (17)$$

where $\chi = \rho_s/\rho_p$ is the ratio of the densities. Then, ΔTTV_p expresses the error propagation from ϑ and χ to TTV_p using the total derivative of Eq. 16. We note that in most cases $\frac{1}{\vartheta} - \chi > 0$ and the absolute value can be replaced by normal brackets. This is because (i) in the case of a giant planet $\vartheta \ll 1$, $\chi > 1$ can be expected, and (ii) in the case of an Earth-like planet $\vartheta < 1$ and $\chi \approx 1$ is plausible. If ϑ is known from a direct photometric detection, this equation can be used to determine the *density ratio*.

From Eq. 15 we can eliminate the radii using masses and densities. This gives the formula for determining the mass ratio,

$$\text{TTV}_p = \frac{a_s}{v} \left| \left(\frac{m_s/\rho_s}{m_p/\rho_p} \right)^{\frac{2}{3}} - \frac{m_s}{m_p} \right| = \frac{a_s}{v} \left| \left(\frac{\mu}{\chi} \right)^{\frac{2}{3}} - \mu \right| \quad (18)$$

$$\Delta \text{TTV}_p = \frac{a_s}{v} \left\{ \left[\frac{2}{3\chi^{\frac{2}{3}}\mu^{\frac{1}{3}}} - 1 \right] \Delta\mu - \frac{2\mu^{\frac{2}{3}}}{3\chi^{\frac{2}{3}}} \Delta\chi \right\}. \quad (19)$$

The error propagation analysis shows that Eq. 16 is quite stable against the ambiguity in χ , while Eq. 18 is more sensitive to χ . This means that *the photometric method is better for a size determination than for a mass determination*. This is also demonstrated in Figs. 3 and 4, which plot TTV_p using Eqs. 16 and 18 for different sizes and masses for some discrete values of χ .

2.2. $\chi = 1$ estimations

In the case of the known transits, the χ relative density is unknown. To make an order-of-magnitude estimate or an upper limit of the size and the mass of a hypothetical satellite, we have to choose some value for the density ratio, e.g. $\chi = 1$. This choice leads to

$$\text{TTV}_p \approx \frac{a_s}{v} \vartheta^2 (1 - \vartheta), \quad (20)$$

or

$$\text{TTV}_p \approx \frac{a_s}{v} \left| \mu^{2/3} - \mu \right|. \quad (21)$$

If we assume that $a_s = a_H/3$, these equations contain only one unknown parameter. As the size determination is not too density-dependent (Eqs. 17, 19., Figs. 3, 4), one can expect better results using Eq. 20 for size determination, but Eq. 21 can also be used for a very rough mass estimation.

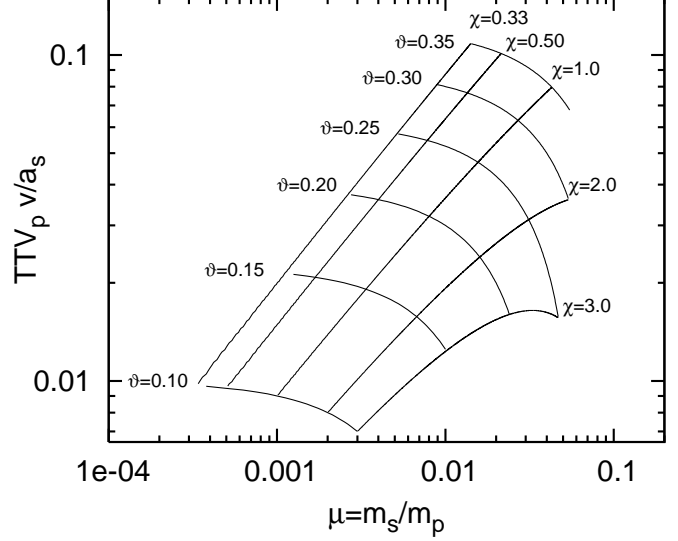


Fig. 5. Grid representation of TTV_p caused by a satellite with different χ density ratios and ϑ size ratios.

2.3. Testing with the Earth-Moon system

A simple test of the calculations described above is to examine the Earth-Moon system. In Szabó et al. (2006) the corresponding numerical calculations are described with the real sizes, orbital periods, and the solar limb darkening also taken into account. The resulting TTV_p is 15.2 minutes (normal amplitude). The corresponding $\text{TTV}_p v/a_s$ is 0.054, when substituting $a_s = a_H/3$.

First we calculated a $\chi = 1$ models leading to the same timing effect. We found that $\vartheta = 0.274$, $\mu = 0.020$. The size of this Moon-model agrees well with the real size of the Moon, and the mass is about twice the real value. This precision is, however, acceptable for a trial estimation for the parameters of an exomoon. However, if we somehow got to know that $\chi = 0.605$ in the Earth-Moon system, we would get an acceptably precise result for both parameters as $\vartheta = 0.253$, $\mu = 0.010$ (Table 1, 2nd row). Both values are concordant with the real parameters within 20%, and suggest the reliability of this method. We conclude that he determined sizes agree with the real properties, and an order-of-magnitude estimate for the mass of the Moon is also possible even when no information on the density assumed.

In order to compare the results $\chi = 1$ estimations to other possible density ratios, a grid presentation of the timing effect is plotted in Fig. 5 based on Eqs. 15 and 18. The lines of constant χ and of constant ϑ values are plotted in the μ vs. $\text{TTV}_p \cdot v/a_s$ space. With this grid one can determine how the mass and the size estimates of the Moon vary if we have a reliable estimation for χ . Also, this grid may help in estimating the size and the mass of a possible exomoon in the case of the positive TTV_p detections of the future.

| | v (km/s) | $1/3a_H$ (10^3 km) | TTV_p (s) | $\text{TTV}_p \cdot v/a_s$ | $\vartheta = \frac{r_s}{r_p}$ | $\mu = \frac{m_s}{m_p}$ |
|----------------|---------------|--------------------------|-----------------------|----------------------------|-------------------------------|-------------------------|
| $\chi = 1$ | 29.8 | 499.6 | 912 | 0.054 | 0.274 | 0.020 |
| $\chi = 0.605$ | 29.8 | 499.6 | 912 | 0.054 | 0.253 | 0.010 |
| real | | | | | 0.272 | 0.012 |

Table 1. Test analysis of the simulated transit light curve of the Earth-Moon system, using data sets with the noise and sampling properties of the Kepler mission.

3. Conclusions

We have presented a novel approach to timing-effect modeling of an exoplanet with a satellite. This approach offers easy calculations with the light curves and helps estimate the mass and the size of a possible satellite. The application to high-precision photometric data, such as is provided by the upcoming satellite missions will lead to estimating the masses and sizes of the moons. The difference between this approach and the SS99-theory is that here we have defined the photometric central time of the transit τ , which accounts for the light curve distortions due to the planet and the satellite, too. Although these seem to be tiny corrections, they have a significant effect in the interpretation of the measurements. An important consequence is that TTV_p cannot exceed a limit if the mass (or the size) of the satellite is increased more and more. To illustrate this, let us imagine a “double planet”, a planet and a satellite having exactly the same size and mass. Because the positions of this “planet” and “satellite” are persistently symmetric, one suspects no timing effect to occur. Our formulation reproduces this result, if we include $\vartheta = \mu = 1$ in Eq. 15.

In Fig. 5, the grid representation of the TTV_p leads to similar conclusions. The constant χ lines at low μ values shows that the bigger the size of a moon, the larger the TTV_p result. But this effect does not increase constantly with size, e.g. a satellite with $\chi = 3$ displays maximal TTV_p if $\mu = 0.034$, and then TTV_p starts decreasing with increasing μ . The constant ϑ lines, on the other hand, show that TTV_p due to a satellite of a fixed size is maximal when the density is low. This is because the barycenter in this system gets closer to the center of the planet, while the photocenter remains at its position regardless of χ . Therefore the distance between the photocenter and the barycenter increases, thus TTV_p increases as well, but never exceeds the time between the transit of the photocenter and the center of the planet.

The limiting values of TTV_p referring to low-density satellites can be calculated from Eqs. 16 and 18 generally and from Eqs. 20 and 21 in the $\chi = 1$ case, and the highest possible value of TTV_p can be calculated. In this case the timing effect is the largest with the value of $v\text{TTV}_p/a_s \approx 0.296$ if $\vartheta = 2/3$ or, what is the same, $\mu = 8/27$. From the viewpoint of the observation, too large an upper estimation of TTV_p is meaningless whenever it exceeds the above limits.

However, a higher value of TTV_p may also be interpreted physically. There are more processes that result in timing effects that can exceed the TTV_p caused by an exomoon. A well-known example is the perturbation of a second planet (Agol & Steffen 2005; Steffen 2006; Gillon et al. 2006; Heyl & Gladman 2006). Ford & Gaudi (2006) suggest that the presence of massive extrojan asteroids can lead to the shift in the transit central time regarding the time of zero radial velocity difference between the planet and the barycenter. The libration, even on a horseshoe orbit, may result in a timing effect that can exceed a few minutes.

The results of this paper can be summarized as follows.

- We gave a theoretical framework for a photometric timing effect caused by moons of extrasolar planets during transits. We included the photometric processes due to the moon via summing the entire photometric signal. This concept offers more parameters to be determined, such as the sizes and/or the masses of the satellites.
- The results are supported by the numerical simulations of Szabó et al., and another simple test is described here. With the analysis of the simulated transits of the Earth-Moon system in front of the Sun, we could almost reproduce the parameters of our Moon exactly.
- We argued that the size of an exomoon is a better predictable parameter than its mass, and we suggest using this estimation in further analyses.

4. Acknowledgements

The research was supported by Hungarian OTKA Grant T042509. GyMSz was supported by the Magyary Zoltán Higher Educational Public Foundation. We thank our referee H. Deeg for helping revise this paper.

References

- Agol, E., Steffen, J., 2005, MNRAS 359, 567
 Bakos, G.A., Knutson, H., Pont, F. et al., 2006, ApJ, 650, 1160
 Barnes, J.W., O’Brien, D.P., 2002, ApJ, 575, 1087
 Charbonneau, D., Winn, J.N., Latham, D. W. et al., 2005, ApJ, 636, 445
 Deeg, H.J., 2002, ESA SP-514, 237 (D02)
 Domingos, R.C., Winter, O.C., Yokoyama, T., 2006, MNRAS, 373, 1227
 Ford, E.B., Gaudi, B.S., 2006, ApJL, 652, L137

- Gillon, M., Pont, F., Moutou, C., 2006, *A&A*, 459, 249
- Heyl, J.S., Gladman, B.J., 2006, *MNRAS*, submitted, astro-ph/0610267
- McCullough, P.R., Stys, J.E., Valenti, J.A. et al., 2006, *ApJ*, 648, 1228
- Sartoretti, P., Schneider, J., 1999, *A&AS*, 134, 550 (SS99)
- Steffen, J.H., 2006, PhD dissertation, University of Washington, astro-ph/0609492
- Steffen, J.H., Agol, E., 2005, *MNRAS L*, 364, 96
- Szabó, Gy.M., Szatmáry, K., Divéki, Zs. and Simon, A., 2006, *A&A*, 450, 395